

Article

Swarm Crawler Robots Using Lévy Flight for Targets Exploration in Large Environments

Yoshiaki Katada ^{1,*} , Sho Hasegawa ¹, Kaito Yamashita ¹, Naoki Okazaki ¹ and Kazuhiro Ohkura ²

¹ Department of Electrical and Electronic Engineering, Setsunan University, Osaka 572-8508, Japan; s.hasegawa@gmail.com (S.H.); yamashita.kaito.0.0.0@gmail.com (K.Y.); naoki.okazaki7010@gmail.com (N.O.)

² Graduate School of Advanced Science and Engineering, Hiroshima University, Hiroshima 739-8527, Japan; kohkura@hiroshima-u.ac.jp

* Correspondence: katada@ele.setsunan.ac.jp

Abstract: This study tackles the task of swarm robotics, where robots explore the environment to detect targets. When a robot detects a target, the robot must be connected with a base station via intermediate relay robots for wireless communication. Our previous results confirmed that Lévy flight outperformed the usual random walk for exploration strategy in an indoor environment. This paper investigated the search performance of swarm crawler robots with Lévy flight on target detection problems in large environments through a series of real robots' experiments. The results suggest that the swarm crawler robots with Lévy flight succeeded in the target's discovery in the indoor environment with a 100% success rate, and were able to find several targets in a given time in the outdoor environment. Thus, we confirmed that target exploration in a large environment would be possible by crawler robots with Lévy flight and significant variances in the detection rate among the positions to detect the outdoor environment's target.

Keywords: swarm robot; autonomous mobile robot; random walk



Citation: Katada, Y.; Hasegawa, S.; Yamashita, K.; Okazaki, N.; Ohkura, K. Swarm Crawler Robots Using Lévy Flight for Targets Exploration in Large Environments. *Robotics* **2022**, *11*, 76. <https://doi.org/10.3390/robotics11040076>

Academic Editors: Charalampos P. Bechlioulis and Panagiotis Vlantis

Received: 17 June 2022

Accepted: 19 July 2022

Published: 22 July 2022

Publisher's Note: MDPI stays neutral with regard to jurisdictional claims in published maps and institutional affiliations.



Copyright: © 2022 by the authors. Licensee MDPI, Basel, Switzerland. This article is an open access article distributed under the terms and conditions of the Creative Commons Attribution (CC BY) license (<https://creativecommons.org/licenses/by/4.0/>).

1. Introduction

Swarm robotics (SR) [1–3] has attracted much research interest from several multi-robot system research community researchers. SR has challenged several control tasks [2,4]: aggregation [5–8], formation [9–12], transport [13,14], task allocation [15–18], and navigation [19,20]. These control tasks should be set as complicated or inefficient for a single robot to tackle. Şahin [21] enumerated several criteria (Şahin [21] claimed to use these criteria as a measure of the degree of SR in a particular study) for distinguishing swarm robotics as follows: autonomy, redundancy, simplicity, and homogeneity. The last criterion enhances the second and third criteria. Thus, homogeneous controllers for individuals are desirable for SR systems. In addition, this approach does not assume an explicit leader in swarm robots. Such a homogeneity results in collective behavior.

Our research group mainly focuses on a target detection problem, which we consider a navigation problem. In this control task, robots explore some targets in a given environment. First, a robot finds a target and sends information to a base station via intermediate relay robots. Then, all of the robots share the detection. Therefore, all robots should be “connected” to the base station via wireless networks [22,23].

In our research group, we investigated the communication range and the number of robots required for a wireless sensor network composed of swarm robots to achieve connectivity in the simulated environment [24] and the preliminary experiment [24]. Then, we applied those results to a target detection problem [25] and investigated the small differential wheeled robots' exploration ability and connectivity. As an exploration strategy, we incorporated two types of random walk into swarm robots: one is Brownian walk, which employs the constant step size, and the other is Lévy flight [26], which employs the step size following Lévy probability distribution. We conducted a series of real experiments

in the indoor environment, including a long corridor with two elevator halls, and confirmed that Lévy flight outperformed Brownian walk. We also investigated the search efficiency of the Lévy flight based on nonlinear dynamics in a simulated and a real experiment [27].

A controversy on Lévy flight advantage in animal behavior has continued [28–35]; Lévy flight is considered the optimal search strategy to find scattered food or preys in the vast field. In such an environment, Lévy flight could enhance the exploration in robotics, as well as in biology. Robots with such a high exploration ability could be applied to various scenarios, e.g., reconnaissance, surveillance, offshore exploration, and rescue. In a large field, such as the above scenarios, a high mobility is required for a robot's hardware. Therefore, we employed swarm crawler robots for large fields. To the best of our knowledge, we are the first to investigate the search performance of swarm robots with Lévy flight in a large field.

This paper investigated the search performance of swarm crawler robots with the Lévy flight [25] on target detection problems in large environments through a series of real experiments. We employed the Lévy flight based on probability distribution, widely employed in robotics. The paper is organized as follows. The next section shortly introduces the related works. Section 3 explains the structure of the crawler robots. Section 4 describes Lévy flight. Section 5 describes the controller of the robots and how to implement a random walk in the controller. Sections 6 and 7 show the settings and the results in real experiments in the indoor environment and the outdoor one, respectively. Conclusions are given in the last section.

2. Related Work

In the SR community, Lévy flight, following Lévy distribution described in Section 4, has been recognized as one of the most efficient search strategies for an environment with sparse targets that robots have no prior knowledge of [36–38].

Recently, Lévy flight has been applied not only to a single robot [39,40] but also to swarm robots [36,37,41–44]. In most swarm robots, however, the search performance and the characteristics of Lévy flight have been investigated in simulated environments [36,37,41,45], the experiments with real robots have been quite a few, and the environments were relatively small [42–44,46].

In addition to this, it has been reported in [36,37] that each individual in swarm robots does not follow Lévy distribution due to collision avoidance from other robots, resulting in an inefficient search. Inconsistency of the distribution would occur due to the truncation of Lévy flight in obstacle avoidance, e.g., against walls or enclosures or detecting a target. Khaluf et al. [36] and Nauta et al. [37] introduced the simple communication rule in which a robot tells its neighbors to avoid itself while executing a long flight. Pang et al. [42] proposed adjusting each robot's step size according to the frequency of physical inference, although there would be no guarantee that each robot's adjusted step sizes follow Lévy distribution.

3. Setup for Crawler Robots

Crawler robots (Figure 1) by NEXUS ROBOT were used in this study. The robot chassis (300(W) × 310(D) × 100(H) [mm]) is equipped with four infrared distance sensors and three infrared target detection sensors located at the front and the side of it. The former is for measuring the distance to other robots and walls, and the latter for detecting targets. The maximum detection ranges of the former infrared sensor and the latter infrared sensor are 300 [mm] and 200 [mm]. The robot's processor is the Arduino-compatible microcontroller embedded with ATmega328, 16 MHz clock speed, and 32 KB flash memory, which collects sensory inputs and outputs signals to control two DC motors connected to the crawlers. This processor can proceed with the controller described in Section 5 without delay or halt. The robot is equipped with wireless devices, XBees [47]. XBees, based on ZigBee wireless standard, can compose wireless ad hoc networks, where nodes can communicate with each other via a multi-hop path. An XBee on each robot was set as a router

of the network. As a target, an infrared-emitting ball was employed to make handling easy, which is the official ball for RoboCup Junior [48]. Its infrared rays are distinguishable from those emitted by the distance sensors described above due to the different wavelengths. A camera is located at the front of the chassis, and Raspberry Pi is located within the chassis, distinguishing the boundary from the field of artificial lawn ground. Raspberry Pi outputs signals to the Arduino when it detects the boundary. This classification system was used only for the outdoor environment. The details are described in Section 7.

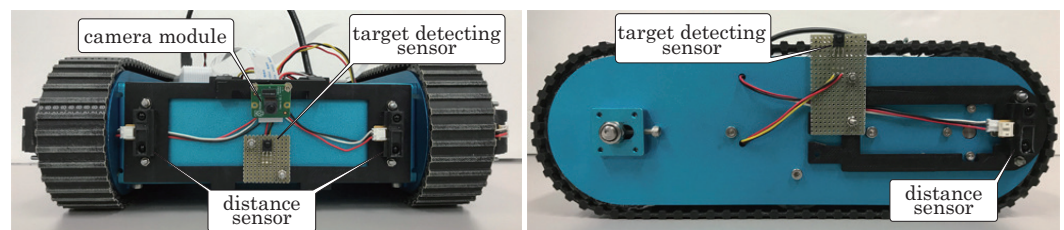


Figure 1. Setup for a crawler robot: (left) Front view. A robot has two infrared distance sensors and an infrared target detection sensor at the front. (right) Side view. A robot has an infrared distance sensor and an infrared target detection sensor on each side.

4. Lévy Flight

A random walk with a constant step size and a random turning angle is well known as Brownian motion. On the other hand, Lévy flight is a random walk whose step size varies according to a Lévy probability distribution [26]. The Lévy probability distribution for a step size, l , is formulated as follows:

$$p_{\alpha,\gamma}(l) = \frac{1}{\pi} \int_0^{\infty} e^{-\gamma q} \cos(lq) dq, \quad \gamma > 0, l \in R \quad (1)$$

where γ is the scaling factor and α ($0 < \alpha < 2$) is a parameter varying the probability distribution shape.

The Lévy probability distribution for a step size can be approximated in the following [49]:

$$p(l) \propto l^{-\alpha} \quad (2)$$

According to the recommendation in [25,39], we define it as follows:

$$p(l) \equiv l^{-1.2} \quad (3)$$

In a computer simulation on a many-target detection problem [50], we compared the performance of Equation (3) with those of the other formulations of the Lévy probability distribution and then confirmed that Equation (3) shows the best performance in the control task. Thus, we employed Equation (3) as a Lévy flight based on the probability distribution in this work.

5. Controller

5.1. Subsumption Architecture

Subsumption architecture (SSA) [51] is employed as a format to describe individuals' behavior of the swarm robots according to our previous work setting [25]. Figure 2 shows a layer structure of SSA implemented in these swarm robots. The SSA used to achieve a control task in target detection problems comprises the following three layers: *transmission*, *obstacle avoidance*, and *target exploration* (these are only for the indoor environment. The SSA for the outdoor environment has an additional layer, described in Section 7). The capital I in a circle in Figure 2 indicates that a lower layer is inhibited when an upper layer is activated. Each layer is composed of some connected modules.

The behavior of each layer can be explained as follows. In the transmission layer, the *detect target* module sends messages to the *transmit messages* module and the *stop* module

when the sensory inputs from the sensors for detecting targets are beyond a threshold. The *transmit messages* module transmits messages to the base station via intermediate relay robots. The *stop* module sends messages to its motors to stop them. In the obstacle avoidance layer, the *detect obstacle* module sends messages to either the *turn right* module or the *turn left* module according to a threshold of the sensory inputs from distance sensors described in Section 3, in order to avoid the obstacles that the robot faces. We tuned those thresholds iteratively by hand until we obtained the desired robot behavior [52]. A random walk, either Lévy flight or Brownian walk, is implemented in the target exploration layer. The details are described in the next subsection. This incremental evolution of the SSA is attractive for the design of collective behavior.

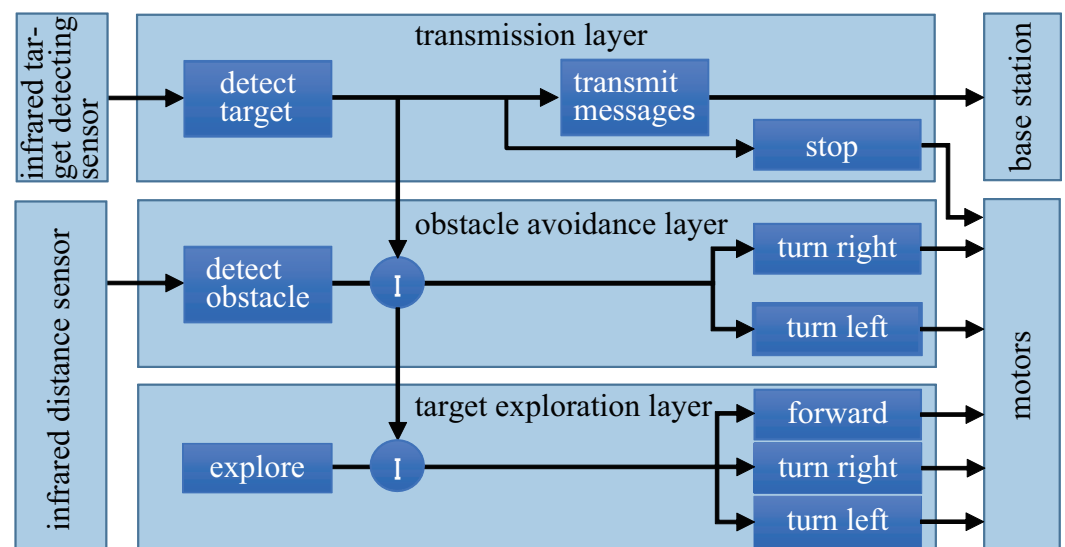


Figure 2. Layer structure of the SSA for the indoor environment. It has three layers: transmission layer, obstacle avoidance layer, and target exploration layer.

5.2. Implementation of a Random Walk in the SSA

In the target exploration layer for Lévy flight described in Section 4, the *explore* module sends messages to one of the following three modules: *forward*, *turn right*, and *turn left*, where *forward* means moving forward and *turn right* (*left*) means rotating clockwise (counter clockwise) at the position.

Lévy flight is implemented by dividing the whole steps into the rotation and move-forward phases. The transition between them occurs at 100%. In the rotation phase, a robot randomly determines the rotation direction and randomly selects an angle of rotation from $\{45, 90, 135\}$ degrees. Then, a robot rotates until it reaches the desired angle (the *turn right* or *turn left* module in Figure 2). A robot moves forward in the move-forward phase, driving two wheels (corresponding to the *forward* module in Figure 2). The movement speed is set to 0.12 m/s for the indoor environment (Section 6) or 0.3 m/s for the outdoor environment (Section 7). The move-forward phase's execution time is a random step size l according to the Lévy probability distribution (Equation (3)) multiplied by l_0 , where l_0 is the movement time per step and was set to 6 sec according to the previous experiment [25]. When an upper layer activation inhibits the target exploration layer, the target exploration layer keeps the residual execution time. After the upper layer inactivation, the target exploration layer is restarted from when it was interrupted. This restart is for maintaining long step sizes generated according to the Lévy probability distribution. This setting is for the consistency of the Lévy probability distribution, described in Section 2.

The Brownian walk followed the same procedure as the Lévy flight except that the move-forward phase's execution time was fixed at 2 s. The setting of rotational angles in the rotational phase was also the same as the Lévy flight.

6. Experiment in Indoor Environment

In Sections 6 and 7, we cope with target detection problems where we assume that robots have no prior knowledge of the environment. In these scenarios, it seems that a random walk is appropriate for the exploration strategy.

We conducted the real experiment in the indoor environment, which is the same as the one employed in our previous work [25,27]. We have two reasons to conduct this experiment: the first is to confirm that the crawler robots' exploration ability with the Lévy flight is equal to or more than the small differential wheeled robots' one [25]. The second is to confirm that the exploration ability of the Lévy flight outperforms the Brownian walk, even when using the crawler robots. In the remainder of this section, we write LF as an abbreviation of Lévy flight and BW as an abbreviation of the Brownian walk, respectively, if necessary.

6.1. Experimental Environment

We investigated the crawler robots' exploration ability with the Lévy flight or the Brownian walk in the building's corridor at Setsunan University (the gray part in Figure 3). There are some classrooms adjacent to this corridor. Thus, the experimental environment is surrounded by walls (we assume that the rooms' doors are closed during the experiment). A target (an infrared-emitting ball (Figure 4 (left)) described in Section 3) was placed at the lower left corner as shown in Figure 3. At the upper right corner, a wireless base station was placed. The base station is a laptop equipped with the same XBee as those on the swarm robots. The XBee equipped on the base station was set as a coordinator. At the beginning of each trial, swarm robots were always placed at the same initial position, the lower right corner, next to the base station (Figure 4 (right)).

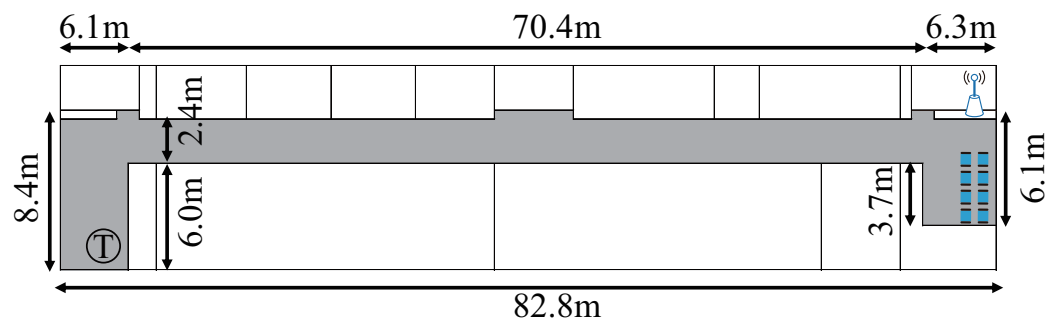


Figure 3. Indoor environment: the capital T in a circle indicates a target at the lower-left corner. A base station is located in the upper-right corner. Swarm robots are initially set in the lower-right corner.



Figure 4. Experimental setup for the indoor environment: (left) infrared ball; (right) initial position of the swarm robots.

6.2. Setting of the Experiment

In this experiment, the swarm robots explore the above environment, detect a target located so far (around 80 [m]) from the base station, and send a message to the base station via intermediate relay robots. We conducted the experiment with eight robots. One trial ended either when the base station receives the message from the robot detecting a target (in the remainder of this paper, the robot detecting a target is considered synonymous with when the base station receives the message from the robot) or when 1800 s (30 min) are performed without receiving the message. As a controller of the swarm robot, the SSA described in Section 5 was employed. We conducted 20 independent runs.

6.3. Experimental Results

Tables 1 and 2 show the time taken for detecting the target in the indoor environment for the LF (this result on the LF was identical to the one obtained in our previous work [27]) and the BW, respectively. The “average” in Tables 1 and 2 indicates the average time for the trials. The “1800” in Table 2 indicates the failure of the trial. Here, the success rate of the LF is exceptionally higher than the BW. This result means that it is difficult for the BW to complete this control task and that the crawler robots with the LF show the search performance, which would be equal to the differential wheeled robots [25].

Figure 5 (left) shows the robot’s expansion in the environment at the end of the trial for the LF. Figure 5 (right) shows the robot detecting the target for the LF.

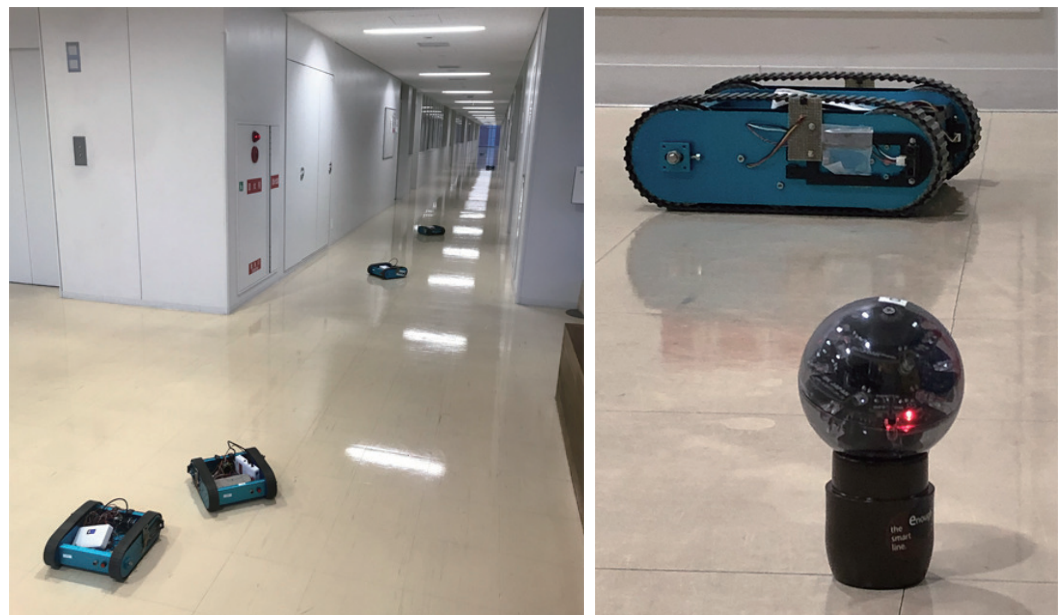


Figure 5. Behavior of the robots for the LF in the indoor environment: (left) expansion of the robots when the robot found the target; (right) detecting the target. Then, the robot stopped and sent a message to the base station.

Table 1. Time taken to detect the target for the LF in the indoor environment.

Trial	Time [s]	Trial	Time [s]	Trial	Time [s]
No.1	953	No.8	1530	No.15	644
No.2	833	No.9	663	No.16	808
No.3	832	No.10	648	No.17	771
No.4	557	No.11	1209	No.18	210
No.5	956	No.12	547	No.19	729
No.6	916	No.13	868	No.20	471
No.7	915	No.14	865	average	796

Table 2. Time taken to detect the target for the BW in the indoor environment.

Trial	Time [s]	Trial	Time [s]	Trial	Time [s]
No.1	1800	No.8	1800	No.15	1800
No.2	1800	No.9	1800	No.16	1800
No.3	1800	No.10	1800	No.17	1800
No.4	1800	No.11	1800	No.18	1800
No.5	1800	No.12	1800	No.19	1800
No.6	1800	No.13	1800	No.20	1800
No.7	1800	No.14	1800	average	1800

7. Experiment in Outdoor Environment

7.1. Experimental Environment

We conducted the real experiment in the artificial lawn ground at Setsunan University (Figure 6). On this ground, the track (the blue area, Figure 7 (left)) surrounds the field (the light and dark green area, Figure 7 (right)). The field is the area to be explored by the robots. The robots must avoid the track to keep within the field because neither boundary walls nor fences surround the track. Thus, we used the camera module controlled by the Raspberry Pi described in Section 3 to distinguish the track from the field. In this experiment, we employed deep convolutional neural networks (CNN) [53] for image classification. The setting of the CNN is described in Appendix A.

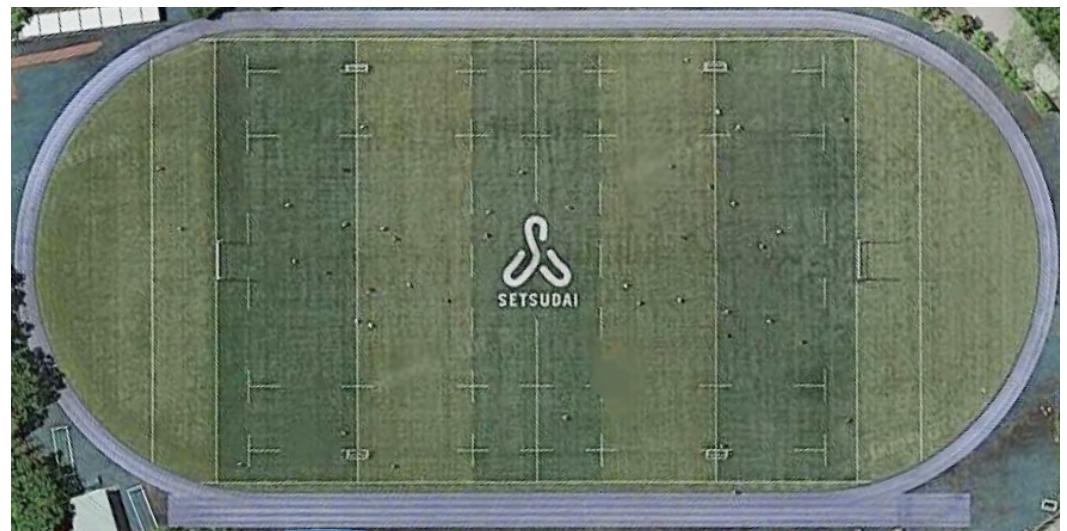


Figure 6. Artificial lawn ground for an outdoor environment. The track (the blue area) surrounds the field (the light and dark green area). Robots explore targets within the field.



Figure 7. Artificial lawn ground images for classification: (left) track image; (right) field image.

Ten targets (infrared-emitting balls described in Section 3 and 6) were placed uniformly over the field (Figure 8). At the lower right corner, a wireless base station was placed. At the

beginning of each trial, the swarm robots were always placed at the same initial position, the lower right corner, next to the base station, at random orientations (Figures 8 and 9).

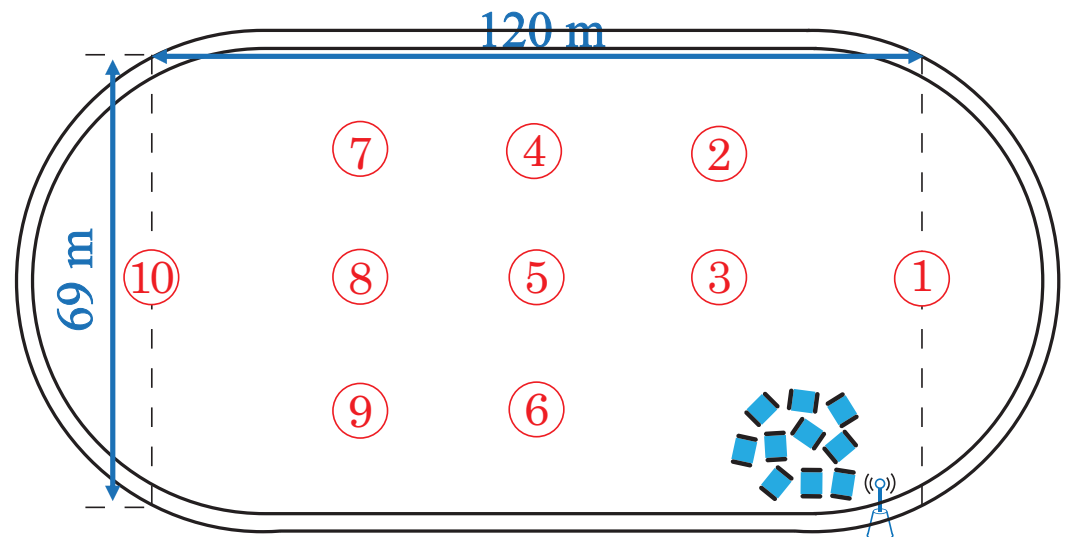


Figure 8. Set up for the outdoor environment. The numbers in circles indicate targets placed uniformly over the field. A base station is located in the lower right corner. Swarm robots are initially set in the lower right.



Figure 9. Initial positions of swarm robots in the outdoor environment.

7.2. SSA for Outdoor Environment

The SSA described in Section 5 was extended for the outdoor environment. We changed the distance threshold to obstacles in the *detect obstacle* module to execute the *turn right* module or the *turn left* module in the outdoor environment. It has an additional layer: *track avoidance* as shown in Figure 10. In the track avoidance layer, the *detect track* module sends messages to the *turn right* module and then to the *forward* module when the camera module detects the track. A robot rotates until it reaches 90 degrees and moves forward in 1 s to avoid the track and then return to the field.

We employed only the Lévy flight for the target exploration layer in this experiment because of the superiority of the Lévy flight to the Brownian walk, which was confirmed in the previous section.

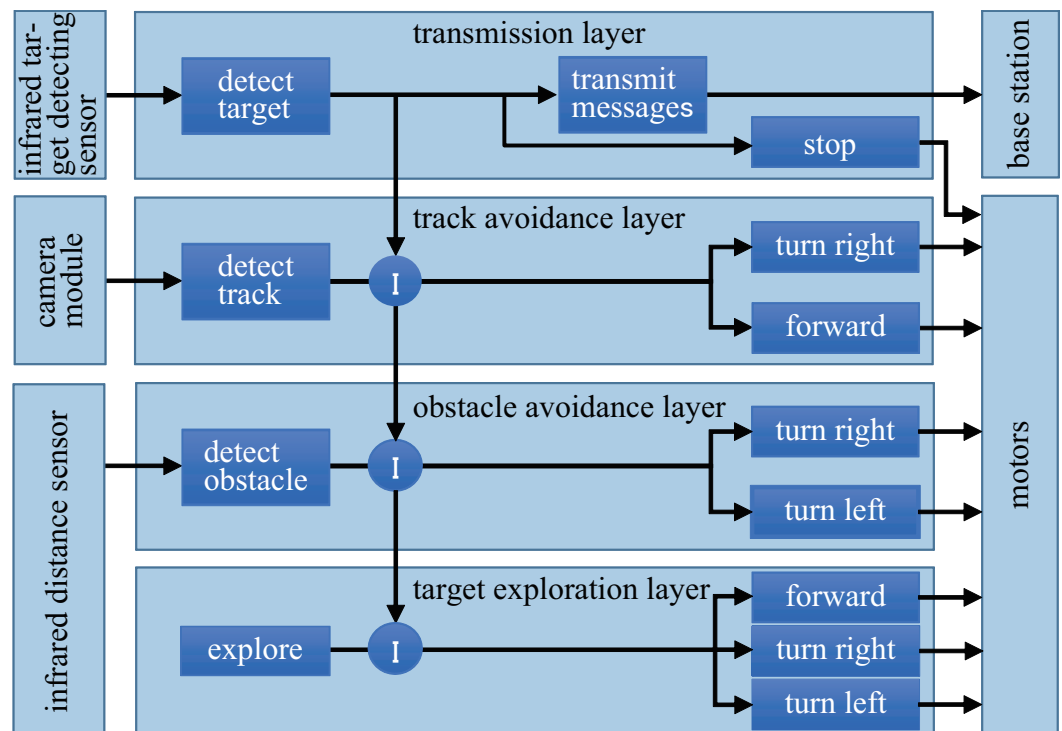


Figure 10. Layer structure of the SSA for the outdoor environment. It has an additional layer, the track avoidance layer, compared to the layers of the SSA for the indoor environment in Figure 2.

7.3. Setting of the Real Experiment

The outdoor environment was much larger than the indoor environment in Section 6. Therefore, we conducted the real experiment in the outdoor environment with ten robots. One trial ended either when the robots detected all the targets or when 1800 s (30 min) was performed without detecting all of the targets. As a controller of the swarm robot, the SSA described in the previous subsection was employed. We conducted 20 independent runs.

7.4. Experimental Results

Table 3 shows the results, including the target detection rate for each trial and each target, and Figure 11 shows the target detection rate for each trial. The robots found 60% of the targets in the best trials. In addition to this, there was no trial where the robots could not detect any target. However, there was a significant fluctuation in the detection rate among the trials. Figure 12 shows the detection rate for each target position. The robots detected the target for each position at least once in the 20 trials. However, the result also shows significant variances among the target positions' detection rates. Here, we can confirm the high detection rates on the center in the longitudinal direction of the environment (①③⑤⑧⑩). Figure 13 shows the robot detecting the target.

Table 3. Target detection for each trial and each position in the outdoor environment: the symbol (○) indicates that the robot found the target placed there.

Trial	Target No.										Detection Rate [%]
	①	②	③	④	⑤	⑥	⑦	⑧	⑨	⑩	
No.1			○	○	○			○	○	○	60
No.2	○		○		○			○		○	50
No.3					○	○					20
No.4					○			○			20
No.5	○		○		○						30
No.6	○				○		○				30
No.7	○	○	○								30
No.8	○				○	○					30
No.9	○										10
No.10				○						○	20
No.11	○		○								20
No.12	○	○			○			○			40
No.13		○	○					○	○		40
No.14	○				○						20
No.15			○					○			20
No.16	○		○		○						30
No.17	○		○	○				○			40
No.18	○	○	○	○	○					○	60
No.19	○							○			20
No.20				○	○					○	30
detection rate [%]	65	20	50	25	60	10	5	40	10	25	31

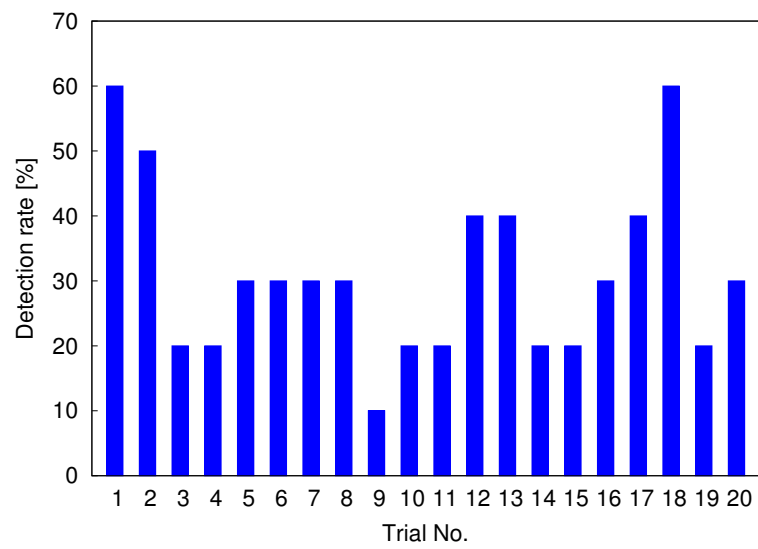


Figure 11. Detection rate for each trial in the outdoor environment.

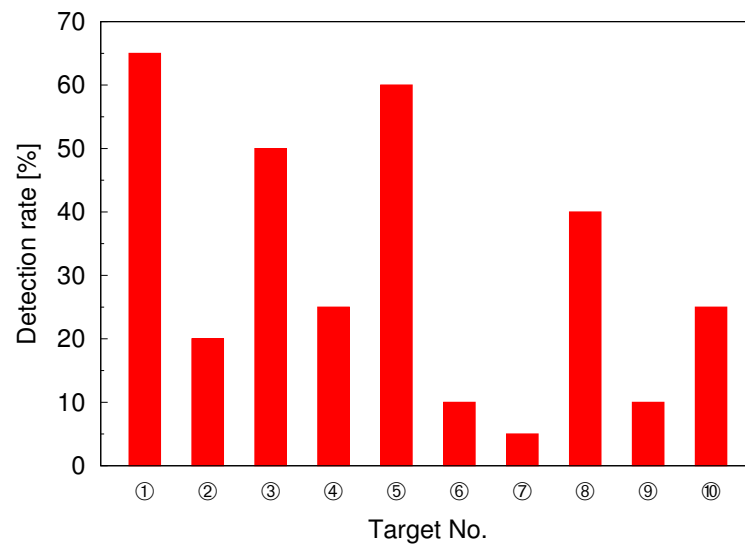


Figure 12. Detection rate for each target in the outdoor environment.



Figure 13. The figure shows a robot detecting the target. Then, the robot stopped and sent a message to the base station after detecting it. Then, the robot restarted its exploration.

7.5. Discussion

We observed the significant variances among the target positions' detection rates described in the previous subsection. These variances were not observed in the result obtained in the computer simulation where many targets were distributed in a simulated environment [50]. For this reason, we consider a hypothesis, which is as follows.

We hypothesize that the target positions' detection rates depend on the periodicity of distance from the center of the robots' initial positions. Figure 14 shows the targets with the virtual concentric circles in the outdoor environment. The center of the concentric circles would be placed near the center of the initial positions of the robots. The smallest circle passes through ①③—the radius is approximately 34.5 [m]. The second and third smallest circles pass through ⑤ and ⑧, respectively. The largest circle passes through ⑩. Those radiuses are approximately 54.0, 75.2, and 102.3 [m]. They are approximately 1.5, 2.1, and 2.96 times as long as the smallest circle's radius. These are the target positions with a low detection rate between the circles, except for ②. Otherwise, we should probably consider ⑤ as an exception, ignoring the second smallest circle. The reason why we suppose this is as follows. As a real experimental procedure, a robot stops its behavior when it detects a target. Then, an experimenter restarts the robot at the beginning of its algorithm after the experimenter removes the detected target. Therefore, the sequence of the behavior in Lévy flight would change after the robot detects the targets.

The variances among the target positions' detection rates demonstrate that it would be better to keep a long flight not only in the case of obstacle avoidance, as mentioned in Sections 2 and 5, but also in the case where robots detect targets to enhance the search performance of the Lévy flight.

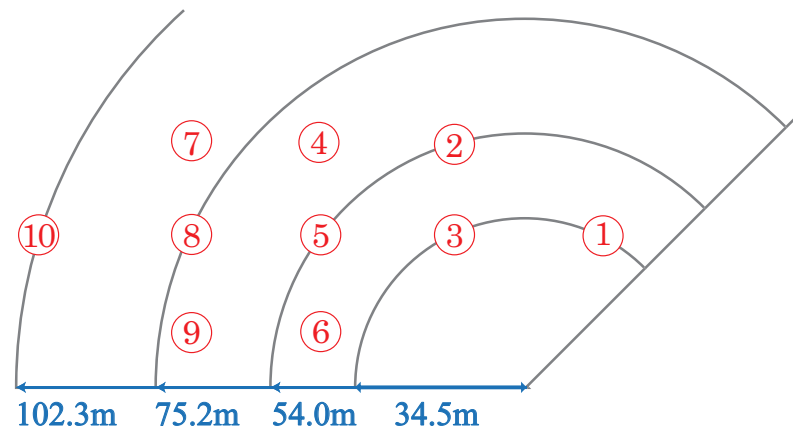


Figure 14. Targets with virtual concentric circles in the outdoor environment. The target numbers are identified with those in Figure 8.

8. Conclusions

The research questions in this paper are: does the Lévy flight's exploration ability outperform the Brownian walk, even when using the crawler robots in indoor environments? Furthermore, can the swarm crawler robots with the Lévy flight detect the targets as uniformly distributed in the outdoor environment? To answer the first research question, we compared the search performance of the swarm crawler robots with the Lévy flight to the one with the Brownian walk in the indoor environment through a series of real experiments. As a result, the swarm crawler robots with the Lévy flight showed a higher target detection rate than those with the Brownian walk in the indoor environment, composed of a long corridor with one target.

To answer the second research question, we investigated the search performance of the swarm crawler robots with the Lévy flight in the outdoor environment. Several targets were uniformly distributed on the artificial lawn in the outdoor environment. The swarm crawler robots with the Lévy flight could detect the target on all of the positions in the 20 trials. The best target detection rate was 60% for each trial. Thus, we confirmed that target exploration in a large environment would be possible by crawler robots with Lévy flight. On the other hand, we observed significant variances among the target positions' detection rates in the outdoor environment, although we did not observe these variances in the result obtained in the computer simulation of our previous work. For this reason, we hypothesized that the target positions' detection rates depend on the periodicity of distance from the center of the robots' initial positions. Therefore, we guess that detecting targets would change the behavior sequence in Lévy flight and not perform well in finding targets for specific positions. This finding in a real environment may improve the proposed method's search performance.

In future works, we will extend our swarm robots' controller with Lévy flight to keep the behavior sequence in Lévy flight even after a robot finds a target. In this paper, the targets were distributed uniformly over the field in the outdoor environment. Thus, we will investigate the search performance of swarm crawler robots with Lévy flight in large environments where targets are distributed heterogeneously, or many clusters are distributed. Finally, we will explore an environment with rough terrain or obstacles.

Author Contributions: Conceptualization, Y.K.; methodology, Y.K.; software, Y.K. and S.H.; validation, Y.K.; investigation, Y.K., S.H., K.Y. and N.O.; resources, Y.K.; data curation, Y.K.; writing—

original draft preparation, Y.K. and K.O.; visualization, Y.K.; supervision, Y.K.; project administration, Y.K. All authors have read and agreed to the published version of the manuscript.

Funding: This research received no external funding.

Institutional Review Board Statement: Not applicable.

Informed Consent Statement: Not applicable.

Data Availability Statement: Not applicable.

Acknowledgments: We thank S. Ichikawa for very useful discussions.

Conflicts of Interest: The authors declare no conflict of interest.

Abbreviations

The following abbreviations are used in this manuscript:

SR	Swarm robotics
SSA	Subsumption architecture
LF	Lévy flight
BW	Brownian walk
CNN	Convolutional neural networks

Appendix A. Convolutional Neural Networks

In the outdoor environment, convolutional neural networks (CNN) were employed as an image classification technique, described in Section 7. We prepared the image dataset for the CNN learning. We operated the crawler robot with the camera module described in Section 3 manually in the artificial lawn ground (Figure 6), gathering the two types of 2000 images: one includes the field, and the other includes the track. Several datasets containing 3500 training images and 500 test images were created by random selection. The learning was conducted in 50 epochs by using mini-batches of training data, where one epoch means a machine learning algorithm has passed over the full training data once. The batch size was set to 35. The performance of the trained CNN for the classification was evaluated against the test data. Table A1 shows the results for training and testing.

Table A1. Performance of the CNN for classification between field and track images.

Training Set		Test Set	
Error	Classification [%]	Error	Classification [%]
2.10×10^{-6}	100	1.49×10^{-2}	99.8

References

1. Trianni, V. *Evolutionary Swarm Robotics*; Springer: Berlin/Heidelberg, Germany, 2008.
2. Brambilla, M.; Ferrante, E.; Birattari, M.; Dorigo, M. Swarm robotics: A review from the swarm engineering perspective. *Swarm Intell.* **2013**, *7*, 1–41. [\[CrossRef\]](#)
3. Hamann, H. *Swarm Robotics: A Formal Approach*; Springer: Berlin/Heidelberg, Germany, 2018.
4. Bayindir, L. A review of swarm robotics tasks. *Neurocomputing* **2016**, *172*, 292–321. [\[CrossRef\]](#)
5. Garnier, S.; Jost, C.; Jeanson, R.; Gautrais, J.; Asadpour, M.; Caprari, G.; Theraulaz, G. Aggregation behaviour as a source of collective decision in a group of cockroach-like-robots. In *Advances in Artificial Life. ECAL2005, Lecture Notes in Computer Science*; Springer: Berlin/Heidelberg, Germany, 2005; Volume 3630, pp. 169–178.
6. Soysal, O.; Bahçeci, E.; Şahin, E. Aggregation in swarm robotic systems: Evolution and probabilistic control. *Turk. J. Electr. Eng. Comput. Sci.* **2007**, *15*, 199–225.
7. Gauci, M.; Chen, J.; Li, W.; Dodd, T.J.; Groß, R. Self-organised aggregation without computation. *Int. J. Robot. Res.* **2014**, *33*, 1145–1161. [\[CrossRef\]](#)
8. Katada, Y. Evolutionary design method of probabilistic finite state machine for swarm robots aggregation. *Artif. Life Robot.* **2018**, *23*, 600–608. [\[CrossRef\]](#)
9. Nouyan, S.; Campo, A.; Dorigo, M. Path formation in a robot swarm—Self-organized strategies to find your way home. *Swarm Intell.* **2008**, *2*, 1–23. [\[CrossRef\]](#)

10. Nouyan, S.; Groß, R.; Bonani, M.; Mondada, F.; Dorigo, M. Teamwork in self-organized robot colonies. *IEEE Trans. Evol. Comput.* **2009**, *13*, 695–711. [[CrossRef](#)]
11. Sperati, V.; Trianni, V.; Nolfi, S. Self-organised path formation in a swarm of robots. *Swarm Intell.* **2011**, *5*, 97–119. [[CrossRef](#)]
12. Shucker, B.; Murphey, T.; Bennett, J.K. Convergence-preserving switching for topology-dependent decentralized systems. *IEEE Trans. Robot.* **2007**, *24*, 1405–1415. [[CrossRef](#)]
13. Groß, R.; Tuci, E.; Dorigo, M.; Bonani, M.; Mondada, F. Object transport by modular robots that self-assemble. In Proceedings of the 2006 IEEE International Conference on Robotics and Automation, ICRA 2006, Orlando, FL, USA, 15–19 May 2006; pp. 2558–2564.
14. Tuci, E.; Groß, R.; Trianni, V.; Mondada, F.; Bonani, M.; Dorigo, M. Cooperation through self-assembly in multi-robot systems. *ACM Trans. Auton. Adapt. Syst.* **2006**, *1*, 115–150. [[CrossRef](#)]
15. Labella, T.H.; Dorigo, M.; Deneubourg, J.L. Division of Labor in a group of robots inspired by ants' foraging behavior. *ACM Trans. Auton. Adapt. Syst.* **2006**, *1*, 4–25. [[CrossRef](#)]
16. Ferrante, E.; Turgut, A.E.; Duñez-Guzmán, E.; Dorigo, M.; Wenseleers, T. Evolution of self-organized task specialization in robot swarms. *PLoS Comput. Biol.* **2015**, *11*, e1004273. [[CrossRef](#)]
17. Pini, P.; Brutschy, A.; Frison, M.; Roli, A.; Dorigo, M.; Birattari, M. Task partitioning in swarms of robots: An adaptive method for strategy selection. *Swarm Intell.* **2011**, *5*, 283–304. [[CrossRef](#)]
18. Ikemoto, Y.; Miura, T.; Asama, H. Adaptive division-of-labor control algorithm for multi-robot systems. *J. Robot. Mechatron.* **2019**, *22*, 514–525. [[CrossRef](#)]
19. Liu, W.; Winfield, A.; Sa, J. A macroscopic probabilistic model of adaptive foraging in swarm robotics systems. In Proceedings of the 6th Vienna International Conference on Mathematical Modelling, Vienna, Austria, 11–13 February 2009.
20. Ducatelle, F.; Di Caro, G.A.; Pinciroli, C.; Mondada, F.; Gambardella, L.M. Communication assisted navigation in robotic swarms: Self-organization and cooperation. In Proceedings of the IEEE/RSJ International Conference on Intelligent Robots and Systems (IROS 2011), San Francisco, CA, USA, 25–30 September 2011; pp. 4981–4988.
21. Şahin, E. Swarm robotics: From sources of inspiration to domains of application. *Lect. Notes Comput. Sci.* **2005**, *3342*, 10–20.
22. Li, J.; Andrew, L.L.; Foh, C.H.; Zukerman, M.; Chen, H.H. Connectivity, coverage and placement in wireless sensor networks. *Sensors* **2009**, *9*, 7664–7693. [[CrossRef](#)]
23. Ghosha, A.; Das, S.K. Coverage and connectivity issues in wireless sensor networks: A survey. *Pervasive Mob. Comput.* **2008**, *4*, 303–334. [[CrossRef](#)]
24. Katada, Y. Connectivity of swarm robot networks for communication range and the number of robots based on percolation theory. In Proceedings of the 2014 IEEE/SICE International Symposium on System Integration, Tokyo, Japan, 13–15 December 2014; pp. 93–98.
25. Katada, Y.; Nishiguchi, A.; Moriwaki, K.; Watakabe, R. Swarm robotic network using Lévy flight in target detection problem. *Artif. Life Robot.* **2016**, *21*, 295–301. [[CrossRef](#)]
26. Lévy, P. *Theorie de L'addition des Variables Aleatoires*; Gauthier-Villars: Paris, France, 1937.
27. Katada, Y.; Yamashita, K. Swarm robots using Lévy walk based on nonlinear dynamics for targets exploration. *Artif. Life Robot.* **2022**, *27*, 226–235. [[CrossRef](#)]
28. Viswanathan, G.M.; Afanasyev, V.; Buldyrev, S.V.; Murphy, E.J.; Prince, P.A.; Stanley, H.E. Lévy flight search patterns of wandering albatrosses. *Nature* **1996**, *381*, 413–415. [[CrossRef](#)]
29. Humphries, N.E.; Queiroz, N.; Dyer, J.R.M.; Pade, N.G.; Musyl, M.K.; Schaefer, K.M.; Fuller, D.W.; Brunnschweiler, J.M.; Doyle, T.K.; Houghton, J.D.R.; et al. Environmental Context Explains Lévy and Brownian Movement Patterns of Marine Predators. *Nature* **2010**, *465*, 1066–1069. [[CrossRef](#)]
30. Nurzaman, S.G.; Matsumoto, Y.; Nakamura, Y.; Shirai, K.; Koizumi, S.; Ishiguro, H. From Lévy to Brownian: A Computational Model Based on Biological Fluctuation. *PLoS ONE* **2011**, *6*, e16168. [[CrossRef](#)]
31. Humphries, N.E.; Weimerskirch, H.; Queiroz, N.; Southall, E.J.; Sims, D.W. Foraging success of biological Lévy flights recorded in situ. *Proc. Natl. Acad. Sci. USA* **2012**, *9*, 7169–7174. [[CrossRef](#)] [[PubMed](#)]
32. López-López, P.; Benavent-Corai, J.; García-Ripollés, C.; Urios, V. Scavengers on the move: Behavioural changes in foraging search patterns during the annual cycle. *PLoS ONE* **2013**, *8*, e54352. [[CrossRef](#)] [[PubMed](#)]
33. Sakiyama, T.; Gunji, Y.P. Emergence of an optimal search strategy from a simple random walk. *J. R. Soc. Interface* **2013**, *10*. [[CrossRef](#)] [[PubMed](#)]
34. Miramontes, O. Lévy flights and self-similar exploratory behaviour of termite workers: Beyond model fitting. *PLoS ONE* **2014**, *9*, e111183. [[CrossRef](#)] [[PubMed](#)]
35. Murakami, H.; Niizato, T.; Tomaru, T.; Nishiyama, Y.; Gunji, Y.P. Inherent noise appears as a Lévy walk in fish schools. *Sci. Rep.* **2015**, *5*, 1–11. [[CrossRef](#)] [[PubMed](#)]
36. Khaluf, Y.; Havermaet, S.V.; Simoens, P. Collective Lévy walk for efficient exploration in unknown environments. In *Artificial Intelligence: Methodology, Systems, and Applications, Lecture Notes in Computer Science*; Springer: Berlin/Heidelberg, Germany, 2018; Volume 11089.
37. Nauta, J.; Havermaet, S.V.; Simoens, P.; Khaluf, Y. Enhanced foraging in robot swarms using collective Lévy walks. In Proceedings of the 24th European Conference on Artificial Intelligence-ECAI, Santiago de Compostela, Spain, 29 August–8 September 2020.

38. Fricke, G.M.; Asperti-Boursin, F.; Hecker, J.; Cannon, J.; Moses, M. From Microbiology to Microcontrollers: Robot Search Patterns Inspired by T Cell Movement. In Proceedings of the ECAL 2013: The Twelfth European Conference on Artificial Life, Sicily, Italy, 2–6 September 2013; pp. 1009–1016.
39. Koyama, H.; Namatame, A. Comparison of efficiency of random walk based search and Levy flight search. *Inf. Process. Soc. Jpn. Tech. Rep.* **2008**, *20*, 19–24. (In Japanese)
40. Nurzaman, S.G.; Matsumoto, Y.; Nakamura, Y.; Shirai, K.; Koizumi, S.; Ishiguro, H. An adaptive switching behavior between Levy and Brownian random search in a mobile robot based on biological fluctuation. In Proceedings of the International Conference on Intelligent Robots and Systems, Taipei, Taiwan, 18–22 October 2010; pp. 1927–1934.
41. Fujisawa, R.; Dobata, S. Lévy walk enhances efficiency of group foraging in pheromone-communicating swarm robots. In Proceedings of the 2013 IEEE/SICE International Symposium on System Integration, Kobe, Japan, 15–17 December 2013; pp. 808–813.
42. Pang, B.; Song, Y.; Zhang, C.; Wang, H.; Yang, R. A swarm robotic exploration strategy based on an improved random walk method. *J. Robot.* **2019**, *2019*, 6914212. [[CrossRef](#)]
43. Sardinha, H.; Dragone, M.; Vargas, P.A. Combining Lévy walks and flocking for cooperative surveillance using aerial swarms. In *Multi-Agent Systems and Agreement Technologies, Lecture Notes in Computer Science*; Springer: Berlin/Heidelberg, Germany, 2020; Volume 12520, pp. 226–242.
44. Cao, M.-L.; Meng, Q.-H.; Luo, B.; Zeng, M. Experimental comparison of random search strategies for multi-robot based odour finding without wind information. *Austrian Contrib. Vet. Epidemiol.* **2015**, *8*, 43–50.
45. Keeter, M.; Moore, D.; Muller, R.; Nieters, E.; Flenner, J.; Martonosi, S.E.; Bertozzi, A.L.; Percus, A.G.; Levy, R. Cooperative search with autonomous vehicles in a 3D aquatic testbed. In Proceedings of the American Control Conference (ACC), Montreal, QC, Canada, 27–29 June 2012; pp. 3154–3160.
46. Sutantyo, D.; Levi, P.; Möslinger, C.; Read, M. Collective-adaptive Lévy flight for underwater multi-robot exploration. In Proceedings of the 2013 IEEE International Conference on Mechatronics and Automation, Takamatsu, Japan, 4–7 August 2013; pp. 456–462.
47. XBee, Digi International Inc. Available online: <https://www.digi.com/products/models/xbp24bz7pit-004> (accessed on 10 June 2022).
48. Robocupjunior Soccer Rules 2014. Available online: https://junior.robocup.org/wp-content/uploads/2014Rules/soccer_2014.pdf (accessed on 10 June 2022).
49. Lee, C.Y.; Yao, X. Evolutionary programming using mutations based on the Lévy probability distribution. *IEEE Trans. Evol. Comput.* **2004**, *8*, 1–13. [[CrossRef](#)]
50. Katada, Y. Swarm robotic network using Lévy flight for exploration—computer simulation for sweeping. *Trans. Soc. Instrum. Control. Eng.* **2018**, *54*, 22–30. (In Japanese) [[CrossRef](#)]
51. Brooks, R.A. A robust layered control system for a mobile robot. *IEEE J. Robot. Autom.* **1986**, *2*, 14–23. [[CrossRef](#)]
52. Brooks, R.A. A Robot that Walks; Emergent Behaviors from a Carefully Evolved Network. *Neural Comput.* **1989**, *1*, 253–262. [[CrossRef](#)]
53. Krizhevsky, A.; Sutskever, I.; Hinton, G. ImageNet classification with deep convolutional neural networks. In Proceedings of the 25th International Conference on Neural Information Processing Systems, Red Hook, NY, USA, 3–6 December 2012; Volume 1, pp. 1097–1105.